Available online at www.sciencedirect.com
ScienceDirect
Journal of Power Sources 160 (2006) 536–541
JOURNAL OF POWER SOURCES
www.elsevier.com/locate/jpowsour

A novel composite negative electrode consist of multiphase Sn compounds and mesophase graphite powders for lithium ion batteries

Ting Fang [a], Li-Yin Hsiao [a], Jenq-Gong Duh [a,*], Shyang-Roeng Sheen [b]

[a] *Department of Material Science and Engineering, National Tsing Hua University, 101, Section 2 Kuang Fu Road, Hsinchu 300, Taiwan*
[b] *Research Center for Applied Science, Academia Sinica, 128, Section 2 Academia Road, Nankang, Taipei 115, Taiwan*

Received 30 October 2005; received in revised form 31 December 2005; accepted 5 January 2006
Available online 24 February 2006

Abstract

A modified electroless plating technique was adopted to prepare the Sn compounds/mesophase graphite powders (MGP) composite electrode. Characterization of the composite material showed that multiphase Sn compounds were uniformly deposited on MGP. The multiphase composition which contained metallic Sn, SnP_3 and SnP_2O_7 were expected to provide a higher spectator to Sn ratio for improved cycleability. During cycling between 0.001 and 1.5 V, the charge capacity was greatly enhanced without appreciable fading. From the voltage profiles and cyclic voltammetry (CV) curves, it was revealed that the capacity fading was caused by either the formation of insulated LiP in the early stage or by aggregation of metallic Sn after prolonged cycling. For improving the cycleability, the cut-off voltage was lowered from 1.5 to 0.9 V. Adjusting the voltage range was manifested to be an effective way for obtaining superior cycling performance in the Sn–P–O/MGP composite negative electrode. The capacity retention was as high as 96% of the highest capacity after charge/discharge between 0.001 and 0.9 V for 45 cycles.

Keywords: Sn; Mesophase graphite powders; Composite negative electrode; Electroless plating

1. Introduction

Graphitic carbons are widely used in commercial Li ion batteries owing to its low potential plateau, acceptable capacity and low cost. Among these, the mesophase graphite is the most popular one due to its stable cycling performance. Although carbon can be lithiated to form LiC_6 which exhibits a theoretical capacity of 372 mAh g^{-1}, the reversible capacity is only around 280–320 mAh g^{-1} [1,2]. To develop negative electrode materials with higher specific capacity, tin-based compounds have been extensively investigated in the past years. Several types of tin compounds have received a great interest, such as metallic Sn [3,4], Sn oxides [5–7], Sn-based alloys [8–11], Sn phosphides [12,13] and Sn phosphates [14–16]. These novel negative electrode materials exhibit superior initial capacity than carbonaceous materials, however, they mostly suffer from rapid capacity fading. The poor cycleability is mainly caused by the pulverization of the negative electrode materials which is associated with the large volume change during formation of Li–Sn alloys. Aggregation of Sn in Sn oxides, phosphides and phosphates during cycling is a significant factor of the pulverization in these compounds [15,17,18]. Many researchers are devoted to solve the problem. Recently, Winter and Besenhard summarized that reducing the particle size and deriving a multiphase composition could retard the pulverization problem [19]. Courtney and Dahn reported that the aggregation rate and cluster size in Sn oxides during cycling was related to the voltage range, cycling temperature and the spectator to Sn ratio [17,18,20]. As lithium reacts with tin oxides, tin ions will be reduced to metallic tin and inactive lithium oxides are simultaneously produced. If metallic tin particles disperse well in the inactive matrix, which is called "spectators", the aggregation will be slowed down. Because the higher spectator to tin ratio leads the tin atoms being farther apart, the tin aggregation and capacity fading is expected to be ameliorated. The amount of spectators can be controlled by mixing active Sn compounds with the inactive species, such as B_2O_3/P_2O_5 glasses [18,21], or doping inactive elements (Ca, Ba, Al, etc.) to form tin-based composite oxides [22–24].

More recently, it is discovered that combining ductile carbonaceous materials with the metallic Sn [25–29], Sn oxides

* Corresponding author. Tel.: +886 3 5712686; fax: +886 3 5712686.
E-mail address: jgd@mx.nthu.edu.tw (J.-G. Duh).

0378-7753/$ – see front matter © 2006 Elsevier B.V. All rights reserved.
doi:10.1016/j.jpowsour.2006.01.034

[30–34] and Sn alloys [35–37] could effectively improve the cycling stability. Electrochemical performance of the composite negative electrodes is influenced by the material system, particle size and size distribution of the Sn compounds and the amount of deposited Sn. A favorable composite negative electrode exhibits nano-sized and uniformly distributed tin compounds. In theory, the higher Sn content would lead to higher volumetric capacity. However, the optimal amount of deposited Sn is usually less than 20 wt.%, for composites with excessive Sn contents exhibit unfavorable capacity fading [25–28,30,31,33]. This problem is speculated to be caused by serious aggregation of deposited Sn during cycling. Since it has been reported that reduced particle size and multiphase compositions are beneficial to enhance the capacity retention, it is inferred that the cycleability of carbonaceous negative electrodes coated with high amount of Sn should be improved by depositing several phases of nano-sized Sn compounds on carbon.

In this study, an electroless plating process was adopted to deposit relative high amount of Sn on mesophase graphite powders (MGP). Electroless plating was an efficient method to produce several phases of tin compounds simultaneously. These multiple phases included tin phosphates and tin phosphide, both of which were expected to derive inactive species as buffers in avoiding aggregation of tin during cycling. Furthermore, the deposited tin compounds could be well-controlled to be either nano-sized or amorphous. It is argued that the capacity fading of MGP coated with relative high amount of Sn should be minimized.

2. Experimental

The mesophase graphite powders was a commercial product supported by China Steel Chemical Corporation (CSCC, Taiwan). Composites of MGP and Sn–P–O compounds were prepared by a modified electroless plating process. The starting reagent included tin(II) sulfate ($SnSO_4$, 99%, Riedel-de Haen), sodium hypophosphite ($NaH_2PO_2{\cdot}H_2O$, 95%, Katayama Chemical) and sodium succinate hexahydrate (99%, Hanawa Extra Pure Reagent). Firstly, appropriate amount of $SnSO_4$ and $NaH_2PO_2{\cdot}H_2O$ were dissolved in de-ionized water, mixed and stirred at room temperature to obtain the metal-precursor. The MGP powders were immediately added into the precursor under strong stirring and then continuously heated to 80 °C and aged for 40 min. During the process, sodium succinate hexahydrate was applied as the buffer to adjust the pH value in the solution. After electroless deposition, the modified MGP powders were repeatedly washed with de-ionized water until the pH value reached 7 and then dried at room temperature in vacuum.

Morphology and the distribution of Sn and P on MGP were observed via SEI micrographs and X-ray color mapping with a newly developed field emission-electron probe microanalyzer (FE-EPMA, JXA-8500F, JEOL, Tokyo, Japan). The deposited amounts of Sn and P on MGP were characterized with an inductively coupled plasma-atomic emission spectrometer (ICP-AES, Perkin-Elmer, Optima 3000 DV, USA). The phases were identified with an X-ray diffractometer (XRD, LabX XRD-6000, Shimadzu, Japan) using a wavelength of Cu Kα (λ = 1.5406 Å).

The electrochemical performance of the Sn–P–O/MGP composite negative electrode was examined by two-electrode test cells consisted of the composite electrode, metallic lithium electrode, polypropylene separator and an electrolyte composed of 1 M $LiPF_6$ in EC/DEC (1:1, vol.%). The composite electrode was prepared by coating the ball-milled slurry comprised of Sn–P–O/MGP composite materials (95 wt.%) and PVDF binder (5 wt.%) on an copper foil and by drying the coated electrode at 100 °C for 12 h. The test cells were assembled in a Ar-filled glove box and galvanostatically cycled at the rate of 0.1 and 0.2*C* in the range of 0.001–1.5 and 0.001–0.9 V, respectively. Cyclic voltammetry (CV) measurements were carried out with a potentiostat (Model 263A, EG&G,) at a scanning rate of 0.1 mV s^{-1}.

3. Results and discussion

3.1. Morphology and phase identification of Sn–P–O/MGP composite materials

On the basis of the elemental quantitative analysis results obtained with ICP, Sn (31.2 wt.%) and P (0.472 wt.%) were deposited on MGP after the electroless plating process. Distribution of Sn and P atoms was revealed by X-ray color mapping carried out with a high-resolution FE-EPMA, as shown in Fig. 1, indicating that the two deposited elements are homogeneously dispersed on the MGP matrix. The X-ray diffraction patterns displayed in Fig. 2b demonstrate that the synthesized Sn–P–O/MGP composite material exhibits a multiphase composition. It is composed of metallic tin, SnP_3 and SnP_2O_7. All of these deposited tin-based compounds are able to be reversibly lithiated and delithiated [12–17,19,28,31,37]. The metallic tin can react with lithium to form various Li–Sn alloys according to the following formula [5–7,17,19,23]:

$$\mathrm{Sn} + x\mathrm{Li}^+ + x\mathrm{e}^- \leftrightarrow \mathrm{Li}_x\mathrm{Sn}\ (0 \le x \le 4.4) \quad (1)$$

As for tin phosphide, Kim et al. [12] revealed the reaction mechanism of Sn_4P_3 by in situ XRD and X-ray absorption spectroscopy. It was suggested that during the first lithiation, Li ions inserted into the Sn_4P_3 layered structure and various phases of Li_xP and metallic Sn were formed between 0.8 and 0.6 V. The decomposition of Sn_4P_3 was irreversible. In this study, the cycling mechanism of SnP_3 is believed to be similar to that of Sn_4P_3 as described above and can be presented as follows:

$$\mathrm{SnP_3} + 3x\mathrm{Li}^+ + 3x\mathrm{e}^- \rightarrow \mathrm{Sn} + 3\mathrm{Li}_x\mathrm{P} \quad (2)$$

On the other hand, Xiao et al. [15] manifested that lithiation of $Sn_2P_2O_7$ at the first cycle involved the decomposition of $Sn_2P_2O_7$ and the formation of metallic tin at 1.3 V. Behm and Irvine [16] announced that SnP_2O_7 exhibited similar position of oxidation/reduction peaks in CV, yet better cycleability as compared with $Sn_2P_2O_7$. The irreversible reaction of SnP_2O_7 with lithium can be expressed as below:

$$\mathrm{SnP_2O_7} + 4\mathrm{Li}^+ + 4\mathrm{e}^- \rightarrow \mathrm{Sn} + \mathrm{Li_3PO_4} + \mathrm{LiPO_3} \quad (3)$$

After the irreversible decomposition, metallic tin atoms dispersed in the inactive Li_3PO_4 and $LiPO_3$ networks. A portion

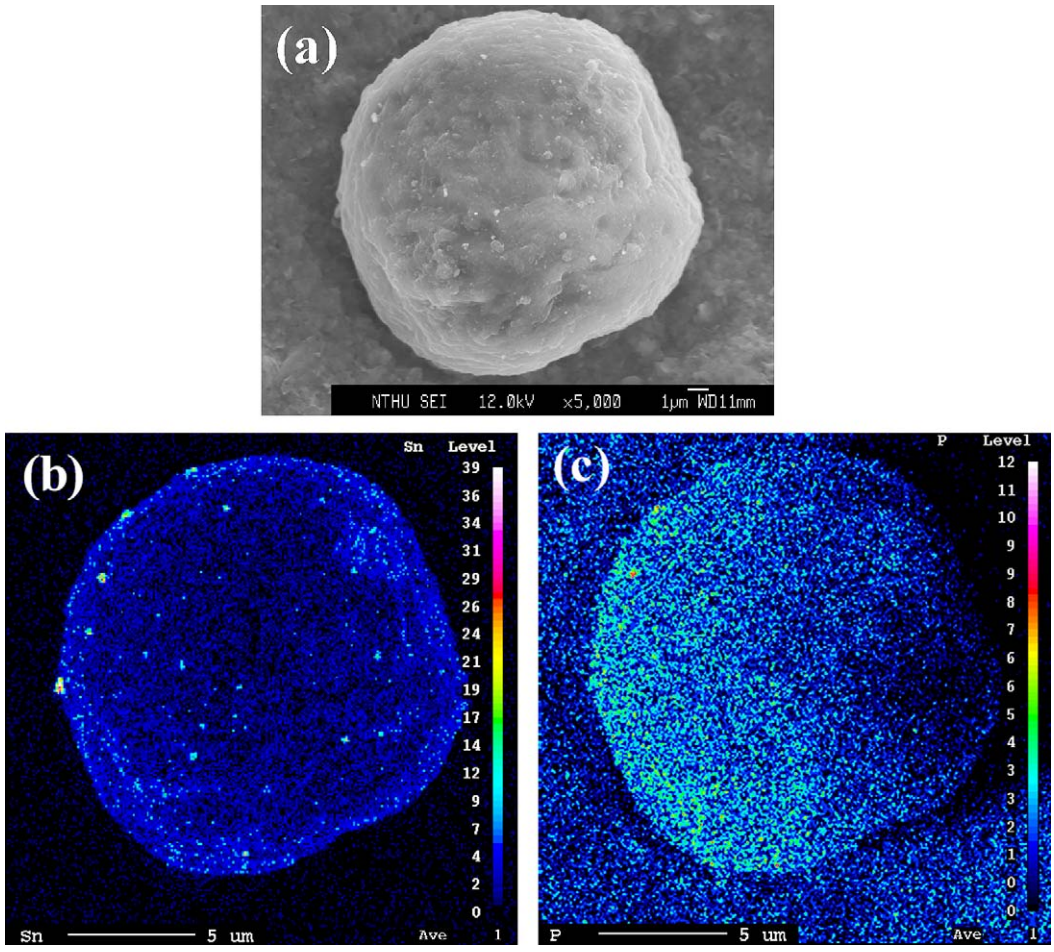

Fig. 1. Micrographs of Sn–P–O/MGP composite material. (a) SEI image, (b) X-ray color mapping for Sn and (c) X-ray color mapping for P.

of LiP derived from the reaction of SnP_3 and lithium (Eq. (2)) were also inactive and could be spectators. Both the primitive and produced metallic tin atoms can further react with lithium to form Li–Sn alloys as described in Eq. (1). The aggregation of Sn during cycling was expected to be retarded owing to the existence of spectators as mentioned above.

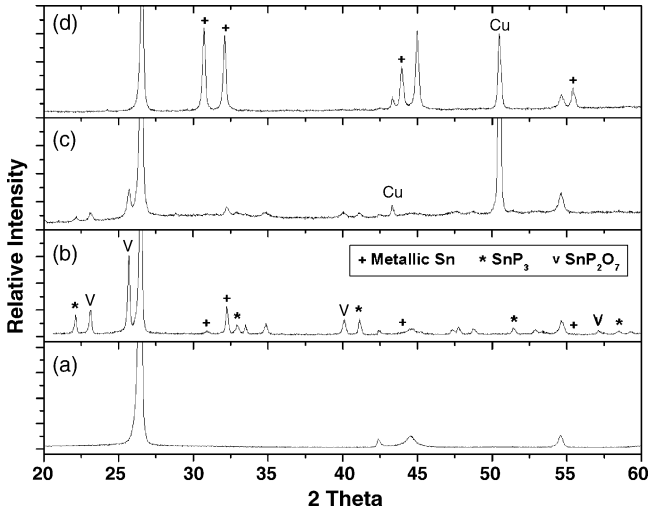

Fig. 2. XRD patterns of: (a) the bare MGP, (b) the Sn–P–O/MGP composite powders, the electrode of Sn–P–O/MGP composite negative electrode (c) before and (d) after the first lithiation/delithiation between 0.001 and 1.5 V at 0.1*C* rate.

The XRD patterns of the composite electrode before and after cycling shown in Fig. 2 reveal that the SnP_3 and SnP_2O_7 phases vanished and a large amount of metallic tin produced after the first cycle. This result was in agreement with those displayed in Eqs. (2) and (3), which were irreversible reactions. Presumably because the particle size of produced Li_xP, $LiPO_3$ and Li_3PO_4 were smaller than the X-ray coherence length, there were no visible diffraction peaks of these spectators in Fig. 2d.

3.2. Electrochemical characterization of Sn–P–O/MGP composite materials

Fig. 3 presents the CV curves of pristine and Sn–P–O deposited MGP in various cycles scanned at 0.1 mV s^{-1} between 0.001 and 1.5 V. The reduction and oxidation peaks in CVs of Sn–P–O/MGP were more complicated than that of MGP. Since the composite negative electrode was a multiphase, the combination of both reduction and oxidation peaks for multiple phases tended to merged into a broadened one.

During the first discharge, a broadened reduction peak was observed until the voltage was reduced to 0.8 V. This indicated the irreversible decomposition of SnP_2O_7 and SnP_3 according to

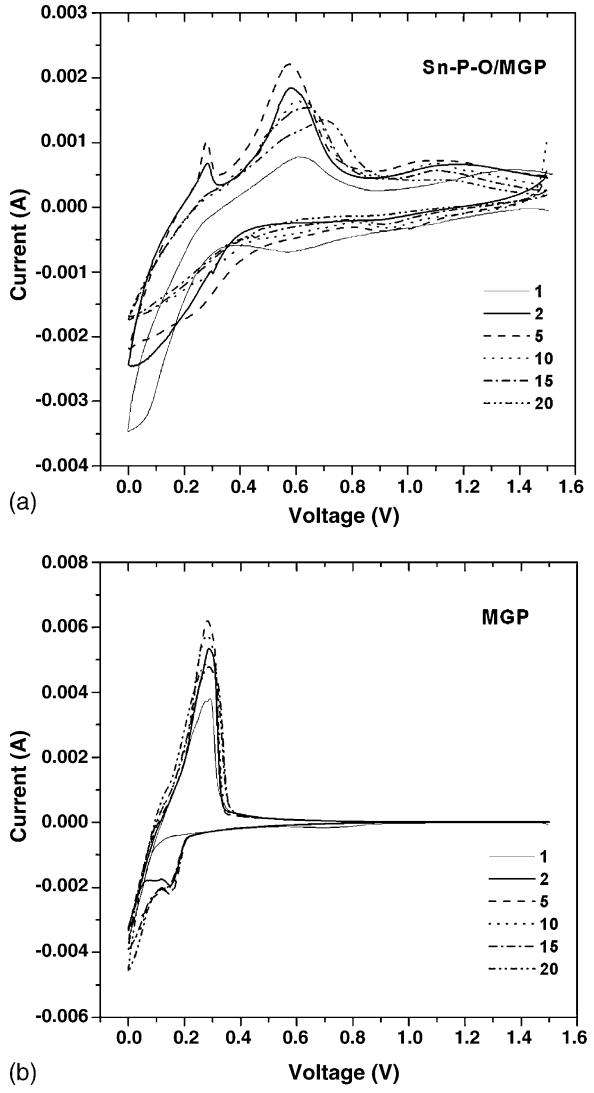

Fig. 3. Cyclic voltammograms of: (a) Sn–P–O/MGP composite material and (b) pristine MGP cycled between 0.001 and 1.5 V at a rate of 0.1 mV s^{-1}.

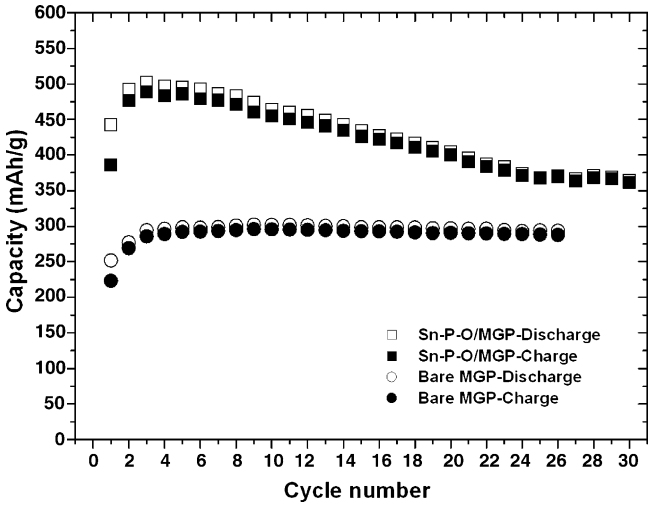

Fig. 4. The capacity retention of Sn–P–O/MGP composite material and pristine MGP cycled between 0.001 and 1.5 V at 0.1*C* rate.

Eqs. (2) and (3), respectively. As lithium being extracted, phase transformation occurred around 0.60 V. This showed that most Li ions were extracted from the Li–Sn alloys [7,31,37]. From the second to the fifth cycle, the pair of reduction/oxidation peaks representing reversible alloying/de-alloying of metallic Sn and Li at around 0.23 V (discharge) and 0.60 V (charge) was enhanced. It was noted that the intensity of the oxidation peak at 0.28 V, caused by delithiation of LiC_6, was also increased. These demonstrated that the lithiation of Sn and carbon was gradually accomplished in the first five cycles. With prolonged cycling, the oxidation peak at 0.28 V was weakened and almost vanished after 10 cycles. This indicated that the activity of carbon to lithium was degraded with cycles. Comparatively, the oxidation peak around 0.6 V still remained distinct in the following cycles. As a result, reactions between metallic Sn and lithium predominated the cycling behavior of the Sn–P–O/MGP composite material. Moreover, in considering the peaks resulted from the formation of Li_3P and LiP at 1.0–0.9 V (reduction) and 1.0–1.2 V (oxidation), respectively, both the transformations were retarded with prolonged cycling.

The cycling performance of the Sn–P–O/MGP composite electrode cycled between 0.001 and 1.5 V at 0.1*C* rate (i.e. 32 mA g^{-1}) is shown in Fig. 4. It manifests that the Sn–P–O/MGP composite electrode exhibit superior electrochemical performance than untreated MGP. Its irreversible capacity at the first cycle was relatively low (57 mAh g^{-1}), while the initial charge capacity was 386 mAh g^{-1}. During the first three cycles, the cell was gradually activated as shown in CV curves and the capacity was raised up to 489 mAh g^{-1} at the third cycle. The activation phenomenon was resulted from incomplete wetting of the electrode by the electrolyte and the capacity was much higher than the highest charge capacity in bare MGP (296 mAh g^{-1}).

Fig. 5 illustrates the charge and discharge curves of bare and Sn–P–O deposited MGP between 0.001 and 1.5 V at 0.1*C* rate. In the first charge curve, there existed three distinct voltage plateaus. It is observed that before the 15th cycle, the charge profiles under 0.9 V exhibited similar shape, while the plateau above 0.9 V gradually became indistinct. This indicated that the capacity fading shown in Fig. 4 in the first 15 cycles was derived from gradual disappearance of the voltage plateau between 0.95 and 1.2 V, which implied the transformation of Li_3P to LiP. After 15 cycles, this plateau almost vanished. Comparing the voltage profiles with the CV results described above, the cause of capacity fading can be revealed. During the initial discharge, lithium inserted into SnP_3 and produced LiP which would be further lithiated to develop the Li_3P phase at 1.0–0.9 V. Li_3P reversibly transformed into LiP as lithium ions were extracted from the hosts between 1.0 and 1.2 V.

Even though Li_3P is a good ionic conductor, LiP is an insulator. As a result, once the amount of LiP increased, the ionic conductivity would be deteriorated. It was argued that owing to the degraded lithium ion conductivity, not all the LiP phase could be lithiated to be Li_3P. In other words, LiP accumulated to a steady state and then the amount of Li_3P was decreased.

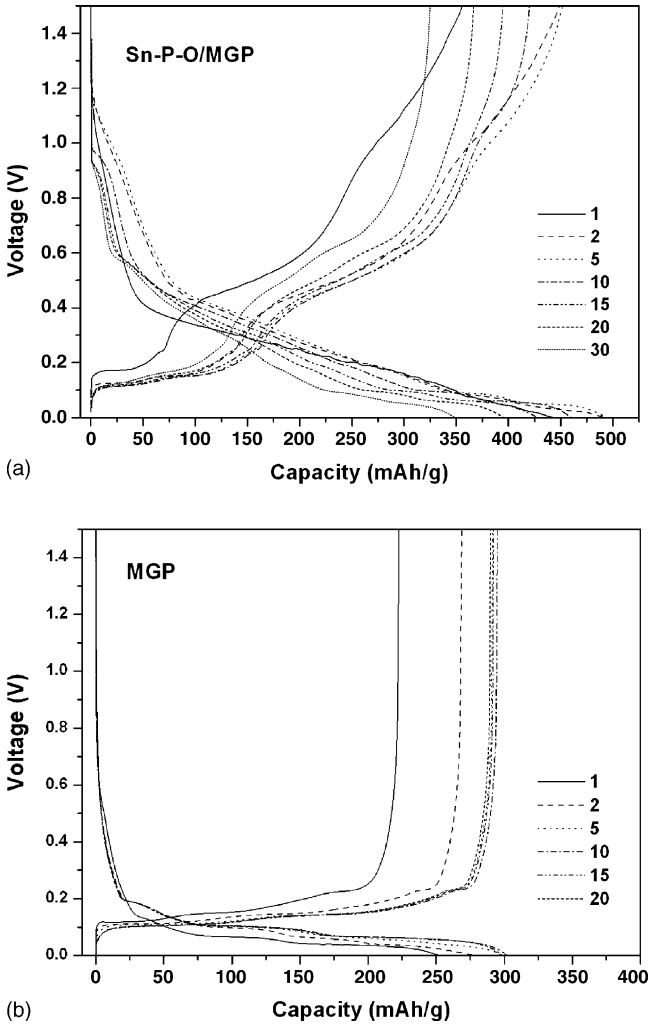

Fig. 5. Charge and discharge curves of: (a) Sn–P–O/MGP composite and (b) pristine MGP cycled between 0.001 and 1.5 V at 0.1*C* rate.

This could be testified by weakening of the formation peaks of Li_3P and LiP shown in Fig. 3a and disappearance of the voltage plateau between 0.95 and 1.2 V presented in Fig. 5a. Consequently, the ionic conductivity was depressed and thus the capacity dropped with increasing LiP.

In this study, the capacity fading was proved to be retarded by the multiphase deposition in the early stage. However, the Sn aggregation was no longer avoidable after prolonged cycling between 0.001 and 1.5 V. As shown in Fig. 3a, the 0.6 V oxidation peak, indicating de-alloying of Sn and Li, became gradually broadened and shifted toward the higher potential. This demonstrated that the aggregation of Sn took place after several cycles. Moreover, the new plateau between 0.6 and 0.7 V after 10 cycles shown in Fig. 5a were also attributed to the aggregation of metallic Sn aggravated the fading. According to Courtney and Dahn's study [20], as the cut-off voltage was higher than 1.3 V, the bonding between the inactive matrix and metallic Sn was destroyed. That is why the electrochemical performance of Sn-based compounds is sensitive to selected voltage window. Even though some spectators, such as LiP, Li_3PO_4 and $LiPO_4$, could

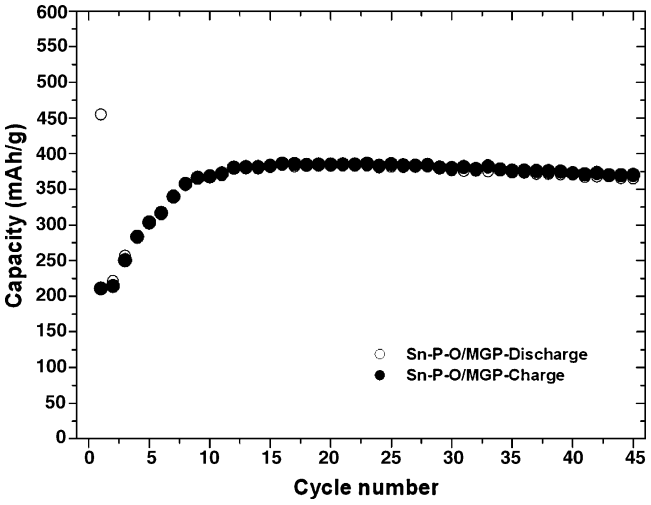

Fig. 6. The capacity retention of Sn–P–O/MGP composite material cycled between 0.001 and 0.9 V at 0.2*C* rate.

be buffers to retard Sn aggregation in the Sn–P–O/MGP composites, the aggregation problem was still encountered.

According to the discussion concerning CVs and voltage profiles, it is believed that if the cut-off voltage was lowered from 1.5 to 0.9 V, the unfavorable phase transformation ($Li_3P \rightarrow LiP + 2Li^+ + 2e^-$) and Sn aggregation could be effectively prevented and the cycleability would be improved. Fig. 6 shows the electrochemical performance of the Sn–P–O/MGP composite electrode cycled between 0.001 and 0.9 V. Although the initial charge capacity was lower (211 mAh g^{-1}) since the voltage plateau above 0.9 V was cut way, the specific capacity was rapidly raised and reached a maximum value of 386 mAh g^{-1} at the 16th cycle. Even after 45 cycles, the capacity remained higher than 370 mAh g^{-1}, which was 96% of the highest capacity.

From the voltage profiles shown in Fig. 7, it is discovered that limiting the cycling potential under 0.9 V not only prevent the capacity loss resulted from formation of LiP, but also successfully avoid the detrimental aggregation of metallic Sn. In other

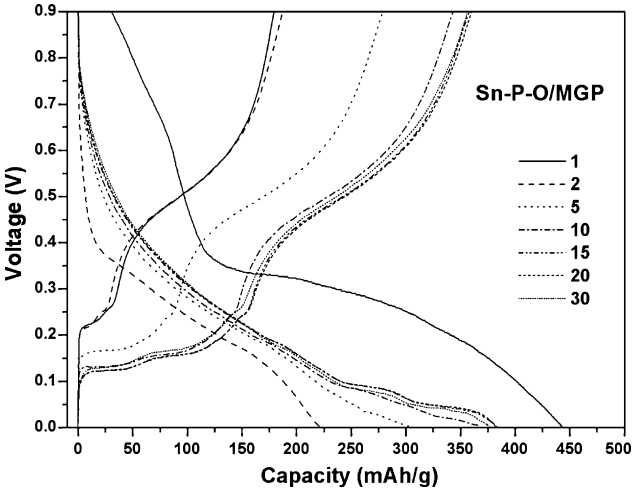

Fig. 7. The charge and discharge curves of multiphase Sn deposited MGP cycled between 0.001 and 0.9 V at 0.2*C* rate.

words, because the lower voltage is not sufficient to destroy the bonding between the inactive networks and metallic tin, the multiphase compounds should provide effective buffers. As a result, in spite of the large amount of deposited Sn (31.2 wt.%), the voltage plateau caused by Sn aggregation failed to show up even after 30 cycles. This favorable capacity retention demonstrates that the composite negative electrode composed of multiphase Sn compounds and MGP exhibits a high capacity along with excellent cycleability under an appropriate cut-off voltage.

4. Conclusions

Multiphase Sn compounds were uniformly plated on MGP to form composite negative electrodes by a modified electroless depositing process. All the phases, including Sn, SnP_3 and SnP_2O_7, were demonstrated to be able to reversibly react with lithium ions during cycling. According to the CV curves and the charge profiles, the fading mechanism of lithium in the Sn–P–O/MGP composite material was proposed. It was discovered that when the voltage window was between 0.001 and 1.5 V, the main cause of capacity fading in the early stage was the formation of insulated LiP from Li_3P in the voltage range of 0.95–1.2 V. After prolonged cycling, the original plateau disappeared and a new plateau associated with aggregation of Sn occurred. Even the composite negative electrode exhibited more rapid capacity fading than bare MGP, its specific capacity remained much higher.

If lowering the cut-off voltage from 1.5 to 0.9 V, the electrochemical performance of the Sn–P–O/MGP composite electrode was greatly improved. Under this reduced potential, the formation of LiP was suppressed and the function of buffers provided by spectators derived from the multiphase Sn compounds prevailed. As a result, the composite negative electrode could exhibit not only higher capacity than pristine MGP, but also favorable capacity retention. A charge capacity higher than 370 mAh g^{-1} after 45 cycles was maintained, and a capacity retention as high as 96% was achieved.

Acknowledgments

This work was mainly supported by the National Science Council, Taiwan, under the contract No. NSC-93-2216-E-007-014. Partial financial assistance from the Ministry of Economic Affairs, Taiwan, under the contract No. 93-EC-17-A-08-S1-003 is also appreciated.

References

[1] T. Ohzuku, Y. Iwakoshi, R. Sawai, J. Electrochem. Soc. 140 (1993) 2490–2498.
[2] D. Aurbach, B. Markovsky, I. Weissman, E. Levi, Y. Ein-Eli, Electrochim. Acta 45 (1999) 67–86.
[3] A.H. Whitehead, J.M. Elliott, J.R. Owen, J. Power Sources 81–82 (2004) 33–38.
[4] W. Choi, J.Y. Lee, B.H. Jung, H.S. Lim, J. Power Sources 136 (2004) 154–159.
[5] N. Li, C.R. Martin, J. Electrochem. Soc. 148 (2001) A164–A170.
[6] M. Mohamedi, S.-J. Lee, D. Takahashi, M. Nishizawa, T. Itoh, I. Uchida, Electrochim. Acta 46 (2001) 1161–1168.
[7] D. Aurbach, A. Nimberger, B. Markovsky, E. Levi, E. Sominski, A. Gedanken, Chem. Mater. 14 (2002) 4155–4163.
[8] E. Rönnebro, J. Yin, A. Kitano, M. Wada, S. Tanase, T. Sakai, J. Electrochem. Soc. 151 (2004) A1738–A1744.
[9] X.-Q. Cheng, P.-F. Shi, J. Alloy Compd. 391 (2005) 241–244.
[10] H. Mukaibo, T. Momma, M. Mohamedi, T. Osaka, J. Electrochem. Soc. 152 (2005) A560–A565.
[11] L. Wang, S. Kitamura, K. Obata, S. Tanase, T. Sakai, J. Power Sources 141 (2005) 286–292.
[12] Y.-U. Kim, C.K. Lee, H.-J. Sohn, T. Kang, J. Electrochem. Soc. 151 (2004) A933–A937.
[13] Y.-U. Kim, S.-I. Lee, C.K. Lee, H.-J. Sohn, J. Power Sources 141 (2005) 163–166.
[14] E. Kim, D. Son, T.-G. Kim, J. Cho, B. Park, K.-S. Ryu, S.-H. Chang, Angew. Chem. Int. Ed. 43 (2004) 5987–5990.
[15] Y.W. Xiao, J.Y. Lee, A.S. Yu, Z.L. Liu, J. Electrochem. Soc. 146 (1999) 3623–3629.
[16] M. Behm, J.T.S. Irvine, Electrochim. Acta 47 (2002) 1727–1738.
[17] I.A. Courtney, J.R. Dahn, J. Electrochem. Soc. 144 (1999) 2045–2052.
[18] I.A. Courtney, W.R. McKinnon, J.R. Dahn, J. Electrochem. Soc. 146 (1999) 59–68.
[19] M. Winter, J.O. Besenhard, Electrochim. Acta 45 (1999) 31–50.
[20] I.A. Courtney, J.R. Dahn, J. Electrochem. Soc. 144 (1999) 2943–2948.
[21] H. Morimoto, M. Nakai, M. Tatsumisago, T. Minami, J. Electrochem. Soc. 146 (1999) 3970–3973.
[22] Y. Idota, T. Kubota, A. Matsufuji, Y. Maekawa, T. Miyasaka, Science 276 (1997) 1395–1397.
[23] Z.-Q. He, X.-H. Li, L.-Z. Xiong, X.-M. Wu, Z.-B. Xiao, M.-Y. Ma, Mater. Res. Bull. 40 (2005) 861–868.
[24] N. Sharma, K.M. Shaju, G.V. Subba Rao, B.V.R. Chowdari, J. Power Sources 139 (2005) 250–260.
[25] B. Veeraraghavan, A. Durairajan, B. Haran, B. Popov, R. Guidotti, J. Electrochem. Soc. 149 (2002) A675–A681.
[26] G.X. Wang, J. Yao, J.-H. Ahn, H.K. Liu, S.X. Dou, J. Appl. Electrochem. 34 (2004) 187–190.
[27] Y. Wang, J.Y. Lee, T.C. Deivaraj, J. Electrochem. Soc. 151 (2004) A1804–A1809.
[28] G.X. Wang, J. Yao, H.K. Liu, S.X. Dou, J.-H. Ahn, Electrochim. Acta 50 (2004) 517–522.
[29] I. Grigoriants, L. Sominski, H. Li, I. Ifargan, D. Aurbach, A. Gedanken, Chem. Commun. 7 (2005) 921–923.
[30] J.Y. Lee, R. Zhang, Z. Liu, J. Power Sources 90 (2000) 70–75.
[31] J.Y. Lee, R. Zhang, Z. Liu, Electrochem. Solid-State Lett. 3 (2000) 167–170.
[32] R. Zhang, J.Y. Lee, Z.L. Liu, J. Power Sources 112 (2002) 596–605.
[33] Y. Wang, J.Y. Lee, B.-H. Chen, Electrochem. Solid-State Lett. 6 (2003) A19–A22.
[34] Y. Wang, J.Y. Lee, J. Power Sources 144 (2005) 220–225.
[35] X.-Z. Liao, Z.-F. Ma, J.-H. Hu, Y.-Z. Sun, X. Yuan, Electrochem. Commun. 5 (2003) 657–661.
[36] Y. Liu, J.Y. Xie, J. Yang, J. Power Sources 119–121 (2003) 572–575.
[37] Z.P. Guo, Z.W. Zhao, H.K. Liu, S.X. Dou, Carbon 43 (2005) 1392–1399.